Protein Structures

DOI: 10.1002/anie.200702161

Ion Mobility–Mass Spectrometry Reveals Long-Lived, Unfolded Intermediates in the Dissociation of Protein Complexes**

*Brandon T. Ruotolo, Suk-Joon Hyung, Paula M. Robinson, Kevin Giles, Robert H. Bateman, and Carol V. Robinson**

Recent applications of mass spectrometry (MS) in structural biology have highlighted its ability to define the stoichiometry of numerous protein complexes.[1,2] When combined with tandem MS, this extra dimension has made possible 1) analysis of polydisperse assemblies,[3] 2) characterization of release of proteins from within proteasome and chaperone complexes,[4,5] and 3) identification of proteins released from intact megadalton ribosomes.[6] Tandem MS is effective because macromolecular protein-complex ions decay through a mechanism that involves a dramatic transfer of charge to monomeric subunits prior to their ejection. This asymmetric dissociation acts to distribute the product ion spectrum over a large m/z range, thus enabling separation of ions with overlapping m/z values and identification of heterocomplexes from released subunits.

It has been proposed that protein unfolding events are involved in the dissociation mechanism,[7–9] although direct evidence pertaining to the structure of the intermediates has not been reported. Ion mobility (IM)–MS,[10,11] a gas-phase technology that separates ions based on their size and shape, has been used to explore gas-phase protein folding,[12–14] oligonucleotide structures,[15] and noncovalent complexes.[16–18] Herein, we apply IM–MS to examine the activated form of a macromolecular complex. For our studies, we used the 56-kDa complex of tetrameric transthyretin (TTR), primarily because its gas-phase dissociation behavior has been studied extensively.[19] Our experiments were performed on a quadropole–ion mobility–time of flight (Q–IM–ToF) instrument (Synapt, Waters, Milford MA, USA, see the Experimental Section) using an IM separator that employs a series of low-voltage DC waves to push ions through a drift chamber filled with neutral molecules (0.5–1 mBar N_2).[20] The speed with which an ion traverses the drift region depends on its collision cross section (CCS); ions with larger CCSs proceed more slowly than ions with smaller ones. These drift times are then calibrated using protein ions of known CCS.[18] Subsequently, molecular modeling is used to generate a range of possible structures, and the CCSs for these models are calculated for comparison with experimental values.

Mass spectra for TTR recorded under conditions designed either to maintain or to activate the intact oligomers (80 V or 150 V accelerating voltage, respectively, in the source region of the instrument) are shown (Figure 1A,C). At 80 V, the minimum accelerating voltage for observation of mass-resolved protein-complex ions, peaks in the spectrum can be assigned to TTR tetramer and octamer. At 150 V, peaks corresponding to the octamer and tetramer persist; however, under these conditions monomeric subunits are also evident (Figure 1C). This result indicates that a population of oligomeric TTR ions is undergoing the initial stages of dissociation and is therefore at an ideal stage for analysis of activated states of the complexes.

IM data shows that without activation, both tetrameric and octameric species exhibit narrow drift-time distributions, thus indicating that the ions exist in a limited range of structural states (Figure 1B). For the activated complexes, a much broader distribution of drift times can be identified (Figure 1D). There are three possible explanations for this observation: 1) peaks at longer drift times are the result of fragmentation of larger oligomeric species after IM separation,[21,22] 2) smaller species (i.e. monomers, dimers, and trimers) created by in-source gas-phase dissociation are observed at m/z values that overlap with the tetramer, or 3) additional extended structures of TTR are formed during activation.

We first considered the possibility of overlap between tetramers and octamers. For example, to overlap with the 15^+ tetramer, an octamer would have to be in the 30^+ charge state. Under the conditions used, the octamer has a predominant charge state of 23^+ (Figure 1A). Moreover, a compact 30^+ octameric ion would appear at shorter drift times than a similarly compact 15^+ tetramer, as the octamer would experience twice the drift field of the tetramer. Hence, we can discount the possibility of overlap between tetrameric and octameric ions. To determine if fragmentation after IM separation could contribute to the broad distribution of arrival times, we set the quadrupole mass filter to transmit only 15^+ tetrameric TTR ions into the drift cell (Figure 1E,G). The IM data recorded for these mass-selected ions at 80 V and 150 V reproduce the narrow and broad arrival-time distributions observed previously (Figure 1F,H). These observations together confirm that the increased drift times observed for 15^+ ions arise neither from dissociation of

[*] Dr. B. T. Ruotolo, S.-J. Hyung, P. M. Robinson, Prof. C. V. Robinson
Cambridge University, Department of Chemistry
Lensfield Road, Cambridge, CB2 1EW (UK)
Fax: (+44) 1223-763-849
E-mail: cvr24@cam.ac.uk
Dr. K. Giles, R. H. Bateman
Waters MS Technologies Centre
Manchester, M23 9LZ (UK)

[**] We gratefully acknowledge M.G. McCammon for assistance in protein expression and purification and funding from the EPSRC and BBSRC. M.G. McCammon and J.L.P. Benesch are acknowledged for critical review.

Supporting information for this article is available on the WWW under http://www.angewandte.org or from the author.

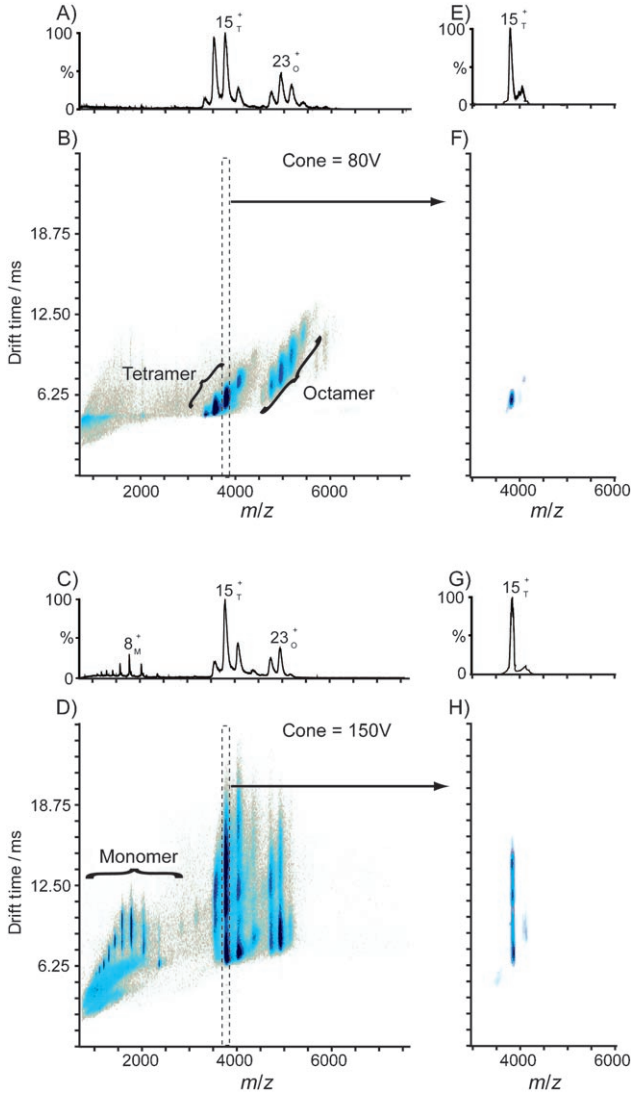

Figure 1. Ion mobility–mass spectrometry data for TTR acquired at cone voltages of 80 V (A, B, E, and F) and 150 V (C, D, G, and H). For both acceleration voltages, the mass spectra (A, C) and drift time versus *m/z* contour plots (B, D) are shown. At 80 V, well-defined charge states of the tetramer $(13–16^+)_T$ and octamer $(20–24^+)_O$ are apparent. The resolution values ($t/\Delta t$) for these features range from 5–8 and are near the performance limit of the ion-mobility separator. At 150 V, the arrival-time distributions observed for tetrameric and octameric ions range from 6.25 to approximately 25 ms. This significant broadening of the arrival time indicates heterogeneous populations of unfolded intermediate structures. Also apparent at low *m/z* values is the appearance of monomeric ions $(6–13^+)_M$, also with broad arrival-time distributions, released from the activated protein complex. For mass-selective experiments, the quadrupole mass analyzer was set to transmit TTR 15^+ ions (*m/z* 3740 ± 10). Mass spectra (E, G) and total arrival-time distribution (F, H) for these mass-selective experiments are shown. A small amount of charge stripping (observed as the 14^+ tetramer ion) is observed, which likely occurs in the ion trap prior to IM separation.

larger oligomers nor from fragmentation after ion-mobility separation; rather, they most likely arise from extended structures of the 15^+ tetramer.

For comparison, arrival-time profiles for four different charge states of tetrameric TTR (13^+–16^+) at a range of acceleration voltages were recorded; the profiles at 200 V are shown (Figure 2). A region common to all four charge states (shaded) can be assigned uniquely to tetrameric ions for the 13^+ and 15^+ TTR charge states. Smaller oligomers with lower charge states contribute to drift-time broadening of the 14^+ and 16^+ tetrameric ions, for example, dimers (7^+ and 8^+), monomers (4^+), and trimers (12^+). Given that the activated tetramers have the highest charge states, their increased drift time over all other oligomers with lower charges must be due to their extended structures. Taken together, the data allow us to conclude that the overall broadening of the drift-time profiles is due to the generation both of multiple conformations (Figure 1) and of smaller overlapping oligomers (Figure 2). Moreover, the drift-time broadening observed for the 13^+ and 15^+ TTR ions is due entirely to conformational effects. This observation is surprising, as these larger structures must be stable in the gas phase for many milliseconds (5–25) to enable their detection under our experimental conditions.

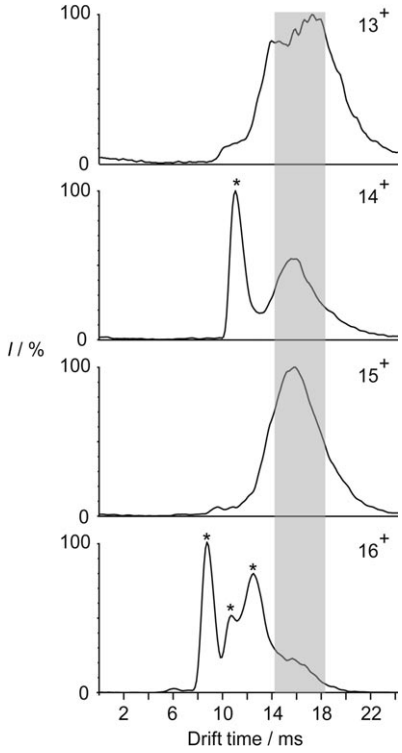

Figure 2. Arrival-time distributions for ions at *m/z* values corresponding to the 13^+ to 16^+ ions of the transthyretin tetramer acquired using 200-V acceleration in the cone region of the instrument. Peaks marked (*) correspond to oligomeric states other than the tetramer. These are indicated by their sharp arrival-time distributions that increase in intensity as acceleration voltage is increased and are not present at *m/z* values known to contain only tetramer (13^+ and 15^+). At the *m/z* value corresponding to the 14^+ tetramer, dimers are observed, and in the case of the 16^+ tetramer, many oligomers are present (monomer, dimer, trimer, and tetramer ions are possible). The shaded area corresponds to the central region of the signal common to all drift-time data and is assigned to activated tetramer ions.

For a detailed analysis of the IM data of the 15^+ tetramer, we converted drift times into CCSs, which are shown as a

function of acceleration voltage (Figure 3). At low activation voltages (80–120 V), the distribution of CCSs is relatively narrow (2900 ± 213 Å^2) and close to the value calculated from the X-ray structure of TTR (3030 Å^2). At 150 V, three distinct

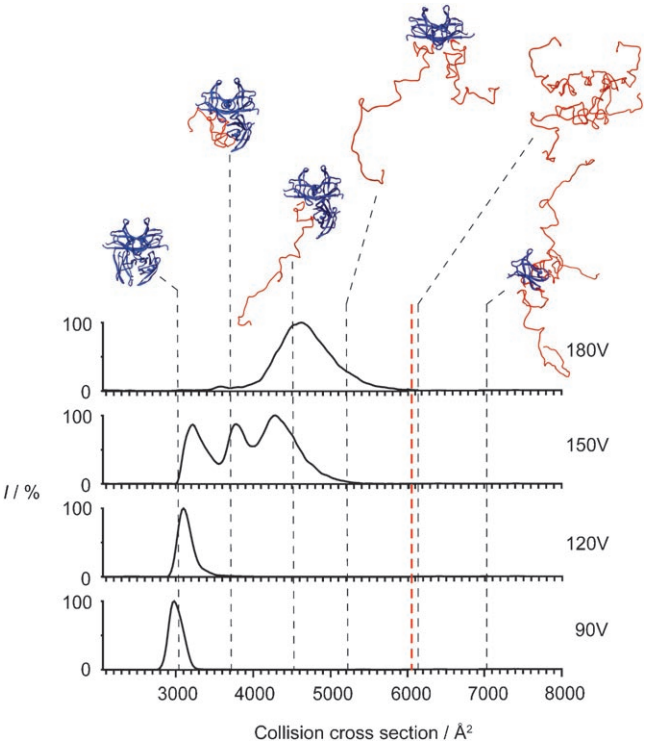

Figure 3. Selected arrival-time distributions, converted into a collision-cross-section axis, for the 15$^+$ charge state of TTR (6000 Å^2 corresponds to approximately 25 ms). Data were acquired at accelerations of 90, 120, 150, and 180 V in the source region of the instrument. Arrival-time distributions at lower and higher accelerating voltages are similar to those shown for 90 V and 180 V, respectively (see the Supporting Information). Superimposed on the data are six selected model TTR structures at various levels of activation. These structures correspond to the crystal structure coordinates (3030 Å^2), one momoner unfolded 21% (3670 Å^2), one monomer 50% unfolded (4514 Å^2), two unfolded monomers at 50 and 30% unfolded (5296 Å^2), four 30% unfolded monomers (6154 Å^2), and three 50% unfolded monomers (7076 Å^2). The red dashed line indicates the cross section of a 100% unfolded monomer docked to a folded transthyretin trimer (6069 Å^2).

populations are evident, corresponding to CCSs of 3200, 3800, 4400 Å^2. At high activation voltage (above 180 V), only a very low population of ions corresponding to tetrameric TTR remains, with CCSs ranging from about 3500 to 5500 Å^2. In summary, measurements of CCS of the 15$^+$ tetrameric TTR at low, medium, and high activation energies reveal well-defined species with low CCS, heterogeneous populations with intermediate values, and a small population with much larger CCS, respectively.

To serve as an initial framework for annotating our data, we generated more than 50 structures using molecular modeling approaches (see Figure 3 and the Supporting Information). These structures were produced both by manually and computationally unfolding transthyretin monomers and docking these unfolded subunits onto the folded complex. Since all topological arrangements of the four transthyretin subunits (i.e. square-planar, linear, tetrahedral) lie within error of our measured value for the tetramer at low activation energies, we only considered model structures containing unfolded monomers for the large ions observed at high acceleration voltages. One, two, three, or all four subunits were allowed to unfold in our simulations, and CCSs for each structure were calculated using Mobcal.[23] From this analysis, we can conclude that no measured CCS values exceed those calculated for a completely extended transthyretin monomer docked onto a folded TTR trimer (red, dashed line Figure 3). Our data are also consistent with model structures in which multiple subunits have undergone partial unfolding; specifically, two, three, or four monomers having unfolded by up to 50, 30, or 20%, respectively, along with structures in which one monomer is unfolded by up to 80%.

Overall, our results show for the first time that activated protein assemblies can populate partially folded intermediate states, which are stable on a millisecond time scale prior to dissociation. These results therefore add to the overall understanding of the dissociation mechanism by providing supporting evidence for a mechanism involving unfolding of one or more subunits to form partially folded intermediate states. More generally, insights into the structures of these intermediates will allow for more precise predictions of the composition of decay products from heterogeneous complexes. This goal is of particular significance for the growing number of applications that rely upon gas-phase dissociation to determine the connectivity and structure of protein interaction networks.[24,25]

Experimental Section

Human transthyretin (concentration 5–10 μM), expressed in *E. coli*[26] was prepared in an aqueous solution buffered to pH 7.0 using 20 mM ammonium acetate. Proteins used for calibration were obtained from Sigma (St. Louis, MO, USA). Nano-electrospray capillaries were prepared as described previously.[27] Pressures and accelerating potentials in the spectrometer were optimized to remove adducts while preserving noncovalent interactions.[28] External calibration of the mass spectra was achieved using solutions of cesium iodide. Errors for all masses reported are within approximately 0.1%.

IM measurements and MS analyses were carried out on a prototype version of a Synapt HDMS system (Waters Corp., Milford, MA) described in detail previously.[20] Briefly, ions are generated by nano-electrospray, guided through the desolvation and quadrupole regions of the instrument, and trapped in an initial traveling-wave ion-guide device (T-Wave) for periods of up to 25 ms. A second T-Wave is operated as an IM separator (maintained at 0.5–1 mBar N_2). Subsequently, ions are directed by a third T-Wave into an orthogonal acceleration time-of-flight (oa-ToF) detector for mass analysis. Since flight times in the MS are much shorter than the transit time of ions in the IM separation device (ca. 250 μs MS flight times versus 20 ms IM transit times), up to 200 spectra can be recorded during the course of each IM separation.

Mobility separation in the traveling-wave device can be controlled by altering the maximum voltage (wave height) and velocity of the traveling waves that propagate through the device. Each measurement was repeated at three different wave heights (8, 10, and 12 V) to optimize the separation characteristics of the IM data. CCS measurements are an average of data acquired at all wave

heights. A wave velocity of 300 m s^{-1} was used throughout. Data presented were acquired with a wave height of 12 V.

For CCS calibration, average drift-time measurements at a single wave height are normalized with respect to charge state. A single, empirically derived, nonlinear correction function is then applied to drift times for calibrant ions from a single protein such that their relative differences correspond to differences recorded for these ions by standard drift-tube techniques.[29,30] This step simultaneously corrects for potential nonlinear relationships between drift time and CCS as well as m/z-dependent flight time after the IM separator.[29] The calibration was then validated using known CCS data from other protein ions. Furthermore, calibrated data were compared to a plot of collision cross section versus molecular weight created using drift-tube[3] and differential mobility analyzer[4] data for low-charge-state protein ions. The average relative precision of the measurements is approximately 4.5%, and the average relative accuracy is approximately 7.5% (including error from the calibration curve and external standards).

Received: May 16, 2007
Revised: July 17, 2007
Published online: September 14, 2007

Keywords: dissociation · electrospray ionization · mass spectrometry · protein structures

[1] J. L. P. Benesch, C. V. Robinson, *Curr. Opin. Struct. Biol.* **2006**, *16*, 245.
[2] A. J. R. Heck, R. H. H. van der Heuvel, *Mass Spectrom. Rev.* **2004**, *23*, 368.
[3] J. A. Aquilina, J. L. P. Benesch, C. S. Slingsby, C. V. Robinson, *Proc. Natl. Acad. Sci. USA* **2003**, *100*, 10611.
[4] M. Sharon, S. Witt, K. Felderer, B. Rockel, W. Baumeister, C. V. Robinson, *J. Biol. Chem.* **2005**, *281*, 9569.
[5] E. van Duijn, D. A. Simmons, R. H. van den Heuvel, H. H. Robert, P. J. Bakkes, H. van Heerikhuizen, R. M. Heeren, C. V. Robinson, S. M. van der Vies, A. J. R. Heck, *J. Am. Chem. Soc.* **2006**, *128*, 4694.
[6] L. L. Ilag, H. Videler, R. C. McKay, F. Sobott, P. Fucini, K. H. Nierhaus, C. V. Robinson, *Proc. Natl. Acad. Sci. USA* **2005**, *102*, 8192.
[7] N. Felitsyn, E. N. Kitova, J. S. Klassen, *Anal. Chem.* **2001**, *73*, 4647.
[8] J. C. Jurchen, E. R. Williams, *J. Am. Chem. Soc.* **2003**, *125*, 2817.
[9] J. L. P. Benesch, J. A. Aquilina, B. T. Ruotolo, F. Sobott, C. V. Robinson, *Chem. Biol.* **2006**, *13*, 597.
[10] G. von Helden, T. Wyttenbach, M. T. Bowers, *Science* **1995**, *267*, 1483.
[11] D. E. Clemmer, M. F. Jarrold, *J. Mass Spectrom.* **1997**, *32*, 577.
[12] E. R. Badman, C. S. Hoaglund-Hyzer, D. E. Clemmer, *Anal. Chem.* **2001**, *73*, 6000.
[13] S. Myung, E. Badman, Y. J. Lee, D. E. Clemmer, *J. Phys. Chem. A* **2002**, *106*, 9976.
[14] S. L. Koeniger, S. I. Merenbloom, D. E. Clemmer, *J. Phys. Chem. B* **2006**, *110*, 7017.
[15] J. Gidden, E. S. Baker, A. Fersoco, M. T. Bowers, *Int. J. Mass Spectrom.* **2005**, *240*, 183.
[16] S. L. Bernstein, T. Wyttenbach, A. Baumketner, J. E. , Shea, G. Bitan, D. B. Teplow, M. T. Bowers, *J. Am. Chem. Soc.* **2005**, *127*, 2075.
[17] J. A. Loo, B. Berhane, C. S. Kaddis, K. M. Wooding, Y. M. Xie, S. L. Kaufman, I. V. Chernushevich, *J. Am. Soc. Mass Spectrom.* **2005**, *16*, 998.
[18] B. T. Ruotolo, K. Giles, I. Campuzano, A. M. Sandercock, R. H. Bateman, C. V. Robinson, *Science* **2005**, *310*, 1658.
[19] F. Sobott, M. G. McCammon, C. V. Robinson, *Int. J. Mass Spectrom.* **2003**, *230*, 193.
[20] S. D. Pringle, K. Giles, J. L. Wildgoose, J. P. Williams, S. E. Slade, K. Thalassinos, R. H. Bateman, M. T. Bowers, J. H. Scrviens, *Int. J. Mass Spectrom.* **2007**, *261*, 1.
[21] C. S. Hoaglund-Hyzer, J. Li, D. E. Clemmer, *Anal. Chem.* **2000**, *72*, 2737–2740.
[22] E. G. Stone, K. J. Gillig, B. T. Ruotolo, K. Fuhrer, M. Gonin, A. J. Schultz, D. H. Russell, *Anal. Chem.* **2001**, *73*, 2233.
[23] M. F. Mesleh, J. M. Hunter, A. A. Shvartsburg, G. C. Schatz, M. F. Jarrold, *J. Phys. Chem.* **1996**, *100*, 16082.
[24] H. Hernandez, A. Dziembowski, T. Taverner, B. Seraphin, C. V. Robinson, *EMBO Rep.* **2006**, *7*, 605.
[25] M. Sharon, T. Taverner, X. I. Ambroggio, R. J. Deshaies, C. V. Robinson, *PLoS Biol.* **2006**, *4*, 267.
[26] Z. H. Lai, W. Colon, J. W. Kelly, *Biochemistry* **1996**, *35*, 6470.
[27] H. Hernández, C. V. Robinson, *Nat. Protocols* **2007**, *2*, 715.
[28] F. Sobott, H. Hernandez, M. G. McCammon, C. V. Robinson, *Anal. Chem.* **2002**, *74*, 1402.
[29] J. L. Wildgoose, K. Giles, S. D Pringle, S. L. Koeniger, S. J. Valentine, R. H. Bateman, D. E. Clemmer, *Proceedings of the 54th Conference of the American Society for Mass Spectrometry*, ThP05, 64.
[30] Clemmer IM Database: http://www.indiana.edu/~clemmer/Research/research.htm.

